Regenerative processes in a radio-frequency Josephson interferometer

A. V. Gusev and V. N. Rudenko

M. V. Lomonosov State University, Moscow
(Submitted 21 March 1984)
Zh. Eksp. Teor. Fiz. **88**, 134–144 (January 1985)

Phase modulation of rf oscillations in a Josephson interferometer with hysteresis is described theoretically outside the plateau in the voltage-current characteristic. A generalized phenomenological model is developed for the magnetic flux quantum jumps in interferometers which treats the phase change produced by external perturbations and fluctuations. The forced oscillations become unstable when the coupling between the interferometer loop and the pumping channel reaches a certain value. The application of this instability to maximizing the sensitivity of quantum rf interferometers (so that the sensitivity is limited only by the constraints imposed by fluctuations in the Josephson contact) is discussed.

Superconducting quantum interferometers (or Squids) are superconducting loops with one or more Josephson junctions. They are employed in experimental physics as sensitive recording elements for measuring weak currents, voltages, electromagnetic fields and gradients, etc.[1] Because they permit relatively easy measurements of unprecedented sensitivity, Squids have found use in fundamental physical experiments concerned with searching for magnetic monopoles,[2] measuring the electric dipole moment of the electron,[3] designing antennas to detect gravitational radiation,[4,5] verifying the equivalence principle,[6] building a "relativistic gyroscope,"[7] etc.

Most of the experiments done so far (including the ones described above) employ single-contact rf Squids with hysteresis, which are the type most commonly found in the laboratory (however, other types such as anhysteretic Squids and constant-current Squids are available[8]). The single-Josephson-junction interferometer is controlled by an oscillating circuit which contains a pump generator. When the amplitude of the forced oscillations exceeds a critical value, jumps between neighboring quantum states occur in the interferometer and the magnetic flux changes discontinuously. The hysteresis losses associated with the magnetic flux reversal decrease the rate of forced oscillation buildup as the pump increases, so that the rf voltage-current (V-I) characteristic of the Squid contains a plateau; two-quantum jumps in the magnetic field give rise to a second plateau, etc. The operating point of the Squid lies on the plateaus; here the external signal (a magnetic flux in the interferometer ring which varies slowly compared to the pumping signal) modulates the amplitude of the forced oscillations of the circuit by an amount which can be measured (if there is a mismatch, the phase is also modulated). The physics of the processes occurring in this conventional type of hysteresis Squid have been studied in detail.[8] In principle, only the thermal noise and the thermal fluctuations of the normal component of the current across the contact resistance should limit the peak sensitivity of this and other types of Squids. In practice, however, the sensitivity is determined by the noise in the coupled electronic circuits and by the difficulties in matching them to the interferometer.[9]

A new type of hysteresic Squid behavior was recently discovered experimentally in Ref. 10—the phase of the forced oscillations is modulated by an amount proportional to the external signal when the pump amplitude lies between adjacent plateaus. The sensitivity measured in Ref. 10 under these conditions was somewhat higher than for the same Squid with conventional amplitude modulation on a plateau. The useful signal also increased as the coupling between the interferometer and the circuit increased.

The purpose of the present work is to find a theoretical explanation for the observed behavior. In order to do this, we generalized the phenomenological magnetic flux jump model developed previously in Ref. 4, in which the jump probability is a function of the measurable external flux (field), by allowing for variations in the time at which the jumps occur. This generalization enabled us to completely describe the Squid behavior, both on and away from the plateaus. The physical interpretation is that even though the average number of hysteresis cycles per unit time is conserved (apart from fluctuations) between the plateaus, the external field can shift the time (phase) of the jump by as much as a circuit oscillation period and thereby modulate the phase of the circuit oscillations. The same mechanism also occurs on a plateau; here, however, it is secondary in importance to the strong modulation of the average number of jumps by the external signal. This mechanism thus becomes important only away from the plateaus.

In addition to providing an interpretation of the experimentally observed hysteresis Squid behavior between adjacent plateaus, the theory predicts destabilization of the forced oscillations between plateaus for certain mismatches and interferometer-circuit coupling factors. We can show that for an underexcited but regenerative Squid, the self-fluctuations in the interferometer may dominate the other types of noise, and in this case the sensitivity of the Squid to magnetic fields will approach the maximum theoretical value.

This paper is organized as follows. We first derive truncated equations for a hysteresis Squid which describe the Squid behavior both on and away from the first plateau (Sec. 1). We then discuss an improved semiphenomenological

 0038-5646/85/010078-06$04.00

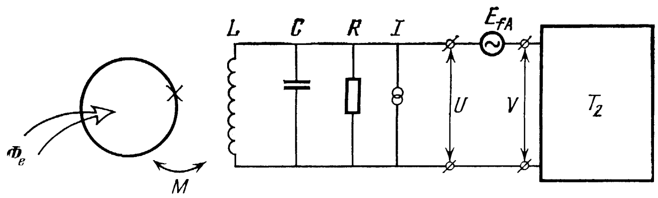

FIG. 1. Equivalent circuit of the rf interferometer; $I = I_0 \sin \omega_t + I_f$, $I_f = I_{fR} + I_{fA}$, where I_{fR} is the thermal resistance current; I_{fA}, E_{fA} are the extraneous fluctuations in the measuring device.

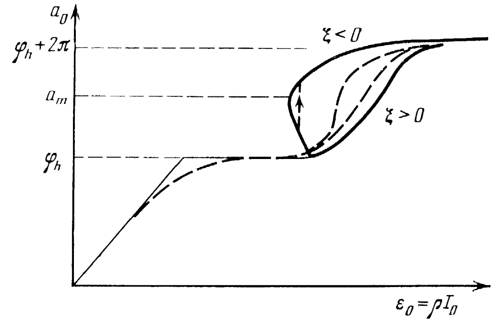

FIG. 2. Change in the voltage-current characteristic between plateaus (the dashed curve gives the characteristic with allowance for fluctuations).

model for the quantum jumps in the magnetic flux in the interferometer (Sec. 2); this will enable us to close the fundamental system of equations. We then analyze the dynamic processes between the first and second plateaus in the *V-I* characteristic in order to find the mismatches and coupling factors for which the Squid parameters are unstable (Sec. 3). Finally, in Sec. 4 we predict and compare the peak sensitivities of hysteresis Squids under various conditions (including the regenerative regime). The analysis is based on the experimental system shown in Fig. 1: L, R, C are the inductance, resistance, and capacitance of the circuit; M is the coefficient of mutual induction between the circuit and the superconducting ring closed by the Josephson junction; the ring inductance L_s is $\gg(\Phi_0/2\pi)I_0^{-1}$: T_2 is the noise temperature of the sensor; $I_p = I_{p0} \sin(\omega t)$ is the pumping current. Figure 2 shows a conventional *V-I* characteristic for a Squid in a fixed external magnetic flux. An operating point on the horizontal portion of the characteristic corresponds to the standard mode of "plateau" operation; the new "off-plateau" regenerative regime occurs when the operating point lies between adjacent plateaus.

1. TRUNCATED EQUATIONS FOR A HYSTERESIS SQUID

If the circuit and the superconducting loop are weakly coupled: $k^2 = M^2/LL_s \ll 1$, the physical processes in the circuit in Fig. 1 are described by the equations

$$\varphi+l\sin\varphi=\varphi_e+\int\varphi_c\,d\tau-li_{fs},\quad l=2\pi L_sI_0/\Phi_0, \tag{1a}$$

$$li_s=\varphi_e+\int\varphi_c\,d\tau-\varphi, \tag{1b}$$

$$\varphi_c''+\varphi_c=-Q^{-1}\varphi_c'+2\Delta\varphi_c+\varepsilon_0\sin\tau-k^2li_s'+\varepsilon_f(\tau), \tag{1c}$$

$$\varphi_V=\varphi_c+e_{fA}. \tag{1d}$$

The notation here is standard: $\varphi = 2\pi\Phi/\Phi_0$ is the internal magnetic flux in the interferometer, divided by the flux quantum Φ_0; $\varphi_c = 2\pi\Phi_c/\Phi_0$ is the rf flux from the circuit; $\varphi_e = 2\pi\Phi_e/\Phi_0$ is the external flux to be measured (it is a linear superposition of the dc bias flux φ_x and the weak, slowly varying signal flux $\tilde{\varphi}_s$). The circuit voltage U is proportional to φ_c:

$$U=\gamma\varphi_c,\quad \gamma=(\Phi_0/2\pi)(\omega/k)(L/L_s)^{1/2}.$$

The remaining symbols are defined by

$$\Delta=(\omega-\omega_c)/\omega,\quad Q\approx\omega RC,\quad \omega_c=(LC)^{-1/2},$$
$$|\Delta|\ll1,\quad \tau=\omega t,\quad \varepsilon_0=\rho I_{p0}\gamma^{-1},$$

The fluctuations in the system are generated by: 1) the thermal noise I_{fs} in the Squid loop ($i_{fs} = I_{fs}/I_0$); 2) noise in the circuit, including the noise current of the preamplifier used to measure the circuit voltage $\mathscr{E}_f = \rho I_f$ ($\varepsilon_f = \rho I_f/\gamma$); 3) the thermal emf E_{fA} of the preamplifier ($e_{fA} = E_{fA}/\gamma$).

We seek a solution of Eqs. (1.1), (1.3) for $l\gg1$ in the form

$$\varphi_c\approx-a\sin(\tau+\vartheta)=-a\sin\psi,\quad |a'/a|,\ |\vartheta'|\ll1, \tag{2a}$$

$$\varphi\approx(\varphi_e+a\cos\psi)/l+\eta(\tau). \tag{2b}$$

The first term in (2b) describes anhysteretic processes, while the second term $\eta(\tau)$ corresponds to the jump-like changes in φ during transitions between neighboring quantum states. We will specify the form of η in Sec. 3.

If we substitute (2b) into (1c) for $l\gg1$, we get the simplified system of equations

$$\begin{aligned} &a'+\delta(a,\varphi_e)a-{}^1/_2\varepsilon_0\sin\vartheta+\chi_a=0,\\ &a\vartheta'+\Delta(a,\varphi_e)a-{}^1/_2\varepsilon_0\cos\vartheta-\chi_\vartheta=0. \end{aligned} \tag{3}$$

Here

$$\begin{aligned} &\delta(a,\varphi_e)=(2Q)^{-1}+\frac{k^2}{2}\bar{\eta}_a(a,\varphi_e),\\ &\Delta(a,\varphi_e)=\Delta-\frac{k^2}{2}-\frac{k^2}{a}\bar{\eta}_\vartheta(a,\varphi_e), \end{aligned} \tag{4}$$

$$\eta_a=\bar{\eta}_a+\tilde{\eta}_a=\langle\eta'\cos\psi\rangle,\quad \eta_\vartheta=\bar{\eta}_\vartheta+\tilde{\eta}_\vartheta=\langle\eta'\sin\psi\rangle,$$

and $\langle\ldots\rangle$ denotes an average over the forced oscillation period; $\bar{\eta}_{a,\vartheta}$ is the statistical average taken over an ensemble of jumps,

$$\begin{aligned} &\chi_a=\varepsilon_a+k^2\tilde{\eta}_a(a,\varphi_e),\quad \chi_\vartheta=\varepsilon_\vartheta+k^2\tilde{\eta}_\vartheta(a,\varphi_e),\\ &\varepsilon_a=\langle\varepsilon_f\sin\psi\rangle,\quad \varepsilon_\vartheta=\langle\varepsilon_f\cos\psi\rangle. \end{aligned} \tag{5}$$

If we linearize (3) with respect to the deviations from the steady-state values a_0, ϑ_0, φ_x, we find the system

$$\begin{aligned} &(p+\delta_1)\tilde{a}-a_0\Delta_0\tilde{\vartheta}=-(C_a\tilde{\varphi}_s+\chi_{a0}),\\ &\Delta_1\tilde{a}+a_0(p+\delta_0)\tilde{\vartheta}=-(C_\vartheta\tilde{\varphi}_s-\chi_{\vartheta0}) \end{aligned} \tag{6}$$

for the deviations $\tilde{a}$ and $\tilde{\vartheta}$ (we use the symbolic notation $p = d/d\tau$); here

$$\delta_0=\delta(a_0,\varphi_x),\quad \Delta_0=\Delta(a_0,\varphi_x),\quad \delta_1=[\partial\delta(a,\varphi_e)a/\partial a]_0,$$

$$\Delta_1=\left[\frac{\partial\Delta(a,\varphi_e)a}{\partial a}\right]_0,\quad C_a=\left[\frac{\partial\delta(a,\varphi_e)a}{\partial\varphi_e}\right]_0,$$

$$C_\vartheta=\left[\frac{\partial\Delta(a,\varphi_e)a}{\partial\varphi_e}\right]_0, \tag{7}$$

$$[\ldots]_0\equiv[\ldots]_{a_0,\varphi_x},\quad \chi_{a0}=\langle\varepsilon_f\cos(\tau+\vartheta_0)\rangle+k^2\bar{\eta}_a(a_0,\varphi_x),$$

$$\chi_{\vartheta0}=\langle\varepsilon_f\sin(\tau+\vartheta_0)\rangle+k^2\bar{\eta}_\vartheta(a_0,\varphi_x).$$

Together with Eqs. (4)–(7), system (3) clarifies how the external perturbation $\tilde{\varphi}_s$ reaches the output of the Squid. The circuit in Fig. 1 is equivalent to a parametric oscillating loop in which the damping and mismatch vary with $\tilde{\varphi}_s$; the transfer coefficients C_α and C_ϑ describe the transfer of the perturbation $\tilde{\phi}_s$ associated with variations in the damping and mismatch, respectively.

According to the linearized system (6), the amplitude and phase variations $\tilde{a}$ and $\tilde{\vartheta}$ of the loop are given by the general expressions

$$\mathrm{Det}\,(p)\tilde{a}=-a_0\{[(p+\delta_0)C_a+\Delta_0C_\vartheta]\tilde{\varphi}_s+(p+\delta_0)\chi_{a0}-\Delta_0\chi_{\vartheta0}\},$$
$$\tag{8}$$
$$\mathrm{Det}\,(p)\tilde{\vartheta}=\{[\Delta_1C_a-(p+\delta_1)C_\vartheta]\tilde{\varphi}_s+\Delta_1\chi_{a0}+(p+\delta_1)\chi_{\vartheta0}\},$$

where

$$\mathrm{Det}\,(p)=a_0\{p^2+(\delta_1+\delta_0)p+\delta_1\delta_0+\Delta_0\Delta_1\}. \tag{9}$$

Equations (8) can be used in principle to estimate the "signal" and the "noise" responses of the Squid, and also to analyze the stability of the circuit in Fig. 1 for a specific choice of the quantities in (7). Before we can do this, however, we must specify the function $\eta(\tau)$ which describes the transitions between neighboring discrete states of the interferometer.

2. MODIFIED MAGNETIC FLUX JUMP MODEL

Equation (2.2) splits the dynamic processes in the interferometer into smooth "hysteresisless" and impulsive components. The latter component can be expressed phenomenologically as a random sequence of pulses

$$\eta(\tau)=2\pi\sum_n\alpha_n[\theta(\psi-2\pi n-\varepsilon_n^+)-\theta(\psi-2\pi n-\varepsilon_n^-)]. \tag{10}$$

Here α_n is a discrete random variable which takes the value $\alpha_n=1$ if a complete hysteresis cycle has occurred (an upward and a downward jump in φ), and $\alpha_n=0$ if there are no jumps; $\theta(\psi)$ is the unit step function; ε_n^+, ε_n^- are the phase shifts, which determine when the jumps occur relative to the timing interval ($\tau_0=2\pi$):

$$\varepsilon_n^+=-\arccos[(b^++\Delta_n^+)/a],\quad \varepsilon_n^-=-\arccos[(b^-+\Delta_n^-)/a],$$
$$b^\pm=\pi\pm\varphi_h-\varphi_e,\quad \varphi_h=(l^2-1)^{1/2}\approx l,\quad l\gg1. \tag{11}$$

The random mutually independent parameters Δ_n^+, Δ_n^- characterize the instability of the leading and trailing edges of the hysteresis pulse associated with thermal noise in the Josephson junction. The present jump model differs from the ones previously suggested in Refs. 4, 8, and 11 (where $\varepsilon_n^+=\varepsilon_n^-=0$) by including the phase shifts ε_n^+, ε_n^-, which contain both a regular and a random component. This ensures a more accurate description both on and beyond the plateau in the rf V-I characteristic. The probability $P\{\alpha_n=1\}$ for a complete hysteresis cycle is readily expressed in terms of the probability P_{KW} calculated by Kurkijarvi and Webb in Ref. 12; indeed,

$$P\{\alpha_n=1\}=P\left\{\left|\frac{b^++\Delta_n^+}{a}\right|\leqslant1,\quad \left|\frac{b^-+\Delta_n^-}{a}\right|\leqslant1\right\}$$
$$\approx P\left\{\left|\frac{b_++\Delta_n^+}{a}\right|\leqslant1\right\}P\left\{\left|\frac{b^-+\Delta_n^-}{a}\right|\leqslant1\right\}$$
$$\approx P\left\{\left|\frac{b^++\Delta_n^+}{a}\right|\leqslant1\right\}$$
$$\approx P\{\Delta_n^+\leqslant a-b^+\}=P_{KW}\left(\frac{a-b^+}{\Delta a}\right). \tag{12}$$

In replacing the product of probabilities in (12) by a single probability, we have used the fact that the probabilities for upward and downward jumps are not symmetric—if the constant bias flux φ_x is negative (to the left of the point $\varphi_{x0}=\pi$) and the flux $\varphi_c(\tau)$ is quasiharmonic, an upward jump will automatically be followed by a downward jump,

$$P\{|(b^-+\Delta_n^-)/a|\leqslant1\,|\,|(b^++\Delta_n^+)/a|\leqslant1\}\approx1.$$

The single parameter

$$\Delta a=l(2\pi\varkappa T/I_0\Phi_0)^{2/3}$$

in the Kurkijarvi-Webb distribution determines the nonzero slope of the plateau in the rf V-I characteristic of the Squid (κ is Boltzmann's constant).

If we recall some standard properties of the delta-function and use (4), (10), we find the expressions

$$\eta_a\approx2\pi\left\langle\sum_n\alpha_n\left\{\frac{b^++\Delta_n^+}{a}\delta(\psi-2\pi n-\varepsilon_n^+)\right.\right.$$
$$\left.\left.-\frac{b^-+\Delta_n^-}{a}\delta(\psi-2\pi n-\varepsilon_n^-)\right\}\right\rangle,$$
$$\tag{13}$$
$$\eta_\vartheta\approx-2\pi\left\langle\sum_n\alpha_n\left\{Z\left(\frac{b^++\Delta_n^+}{a}\right)\delta(\psi-2\pi n-\varepsilon_n^+)\right.\right.$$
$$\left.\left.+Z\left(\frac{b^-+\Delta_n^-}{a}\right)\delta(\psi-2\pi n-\varepsilon_n^-)\right\}\right\rangle,$$

for the stochastic functions defined in (4); here

$$Z(A)=(1-A^2)^{1/2}.$$

Using the standard technique for analyzing periodic time-dependent processes,[12] we find from (13) that

$$\bar{\eta}_a(a,\varphi_e)\approx\overline{\alpha_n\frac{b^+-b^-+\Delta_n^+-\Delta_n^-}{a}}\approx\frac{2\varphi_h}{a}\bar{\alpha}_n,$$
$$\tag{14}$$
$$\bar{\eta}_\vartheta(a,\varphi_e)\approx-\overline{\alpha_n\left[Z\left(\frac{b^++\Delta_n^+}{a}\right)+Z\left(\frac{b^-+\Delta_n^-}{a}\right)\right]}.$$

The averaging in (14) is over the Kurkijarvi-Webb distribution function (12). If we substitute (14) into (4) and write $\xi \equiv 2Q(\Delta - k^2/2)$, we get

$$\delta(a, \varphi_e) \approx (2Q)^{-1}\left\{1 + \frac{2k^2Q}{a^2}(b^+ - b^-)\bar{\alpha}_n\right\},$$

$$\Delta(a, \varphi_e) \approx (2Q)^{-1}\left\{\xi + \frac{2k^2Q}{a}\left[Z\left(\frac{b^+ + \Delta_n^+}{a}\right) + Z\left(\frac{b^- + \Delta_n^-}{a}\right)\right]\Bigg|\, \alpha_n = 1\right\}. \tag{15}$$

We now show that Eq. (8) together with (15) correctly describes the behavior of a conventional rf Squid with operating point (pump amplitude) on the plateau of the rf *V-I* characteristic. Indeed, we have $a \approx b^+ \approx |b^-| \gg 1$, $Z \ll 1$ on the plateau and the influence of the shift mechanism on the circuit oscillations is negligible compared to the effects of the variation in the number of hysteresis pulses. Equations (15) therefore simplify to

$$[\delta(a, \varphi_e)]_{pl} \approx (2Q)^{-1}\left\{1 + \frac{4k^2Q}{a}P_{KW}\left(\frac{a - b^+}{\Delta a}\right)\right\},$$
$$[\Delta(a, \varphi_e)]_{pl} \approx (2Q)^{-1}\xi \tag{16}$$

and yield the estimates

$$(\delta_0)_{pl} \approx (2Q)^{-1}\left\{1 + \frac{4k^2Q}{a}P_0\right\}, \quad (\delta_1)_{pl} \approx 2k^2W_0/\Delta a,$$
$$\Delta_1 \approx \Delta_0 \approx (2Q)^{-1}\xi, \quad C_a \approx 2W_0k^2/\Delta a, \quad C_\vartheta \approx 0,$$
$$P_0 = \left[P_{KW}\left(\frac{a - b^+}{\Delta a}\right)\right]_0, \quad W_0 = \left[\frac{dP_{KW}(x)}{dx}\right]_0 \tag{17}$$

for the equivalent Squid parameters (7). (The zero subscript in these equations indicates quantities evaluated at the steady-state values $a = a_0$, $\varphi_e = \varphi_x$.)

If the mismatch vanishes ($\xi = 0$), the only effect of the weak external perturbation $\tilde{\varphi}_s$ will be to vary the amplitude of the circuit oscillations,

$$(\delta\tilde{a})_{pl} \approx (C_a/\delta_1)_{pl}\tilde{\varphi}_s \approx \tilde{\varphi}_s. \tag{18a}$$

If $\xi \neq 0$, a phase shift $\delta\tilde{\vartheta}$ also occurs and reaches a maximum for some value $\xi = \xi_{\rm opt}$ (Refs. 12–14):

$$\delta\tilde{\vartheta} \approx \left[W_0k^2Q/\Delta a\left(1 + \frac{4k^2Q}{l}P_0\right)\right]^{1/2}\tilde{\varphi}_s,$$
$$|\xi|_{opt} \approx \left[k^2Q\frac{2W_0}{\Delta a}\left(1 + \frac{4k^2Q}{l}P_0\right)\right]^{1/2}. \tag{18b}$$

Equations (18a), (18b) are in agreement with the usual theory for conventional on-plateau Squids.[4,8,11,13,14]

At the same time, Eqs. (8) and (15) satisfactorily describe the steady-state behavior of a Squid, which corresponds to the portion of the characteristic between the first and second plateaus. In this case the frequency of the hysteresis pulses is conserved (up to fluctuations), and the principal effect of the external perturbation $\tilde{\varphi}_s$ is to change their positions in time; Eqs. (15) take the form

$$[\delta(a, \varphi_e)]_{out,\,pl} \approx (2Q)^{-1}\left[1 + \frac{4k^2Q\varphi_h}{a^2}\right],$$
$$[\Delta(a, \varphi_e)]_{out\,pl} \approx (2Q)^{-1}\left\{\xi + \frac{2k^2Q}{a}\left[Z\left(\frac{b^+}{a}\right) + Z\left(\frac{b^-}{a}\right)\right]\right\}; \tag{19}$$

for the dynamic Squid parameters (7), we have

$$(\delta_0)_{out\,pl} \approx (2Q)^{-1}\left[1 + \frac{4k^2Q\varphi_h}{a_0^2}\right],$$
$$(\delta_1)_{out\,pl} \approx (2Q)^{-1}\left[1 - \frac{4k^2Q\varphi_h}{a_0^2}\right]^{1/2}$$
$$\Delta_0 \approx (2Q)^{-1}\xi, \quad \Delta_1 \approx (2Q)^{-1}[\xi + 2k^2Qa_0^{-1}Z_0^{-1}(b^+/a)], \tag{20}$$
$$C_a \approx 0, \; C_\vartheta \approx -a_0^{-1}k^2Z_0^{-1}(b^+/a),$$

outside the plateau. Equations (8) with (20) imply that if $\Delta_0 = \xi = 0$, the only direct effect of the external perturbation $\tilde{\varphi}_s$ will be to modulate the phase of the circuit oscillations; if the final mismatch ξ is $\neq 0$ then the amplitude will also be indirectly modulated. The above model thus explains the experimental results in Ref. 10 at least qualitatively. Allowance for the fluctuations enables us to estimate the sensitivity, i.e., the smallest recordable signal $(\tilde{\varphi}_s)_{\rm min}$. As a preliminary we will first investigate the dynamic behavior of the Squid outside the plateau.

3. DYNAMIC INSTABILITY OF STEADY STATES OUTSIDE THE PLATEAU

We can readily find the steady-state amplitude and phase from Eqs. (3) by omitting the time derivatives and fluctuations,

$$a_0 = \tfrac{1}{2}\varepsilon_0[\delta^2(a_0, \varphi_x) + \Delta^2(a_0, \varphi_x)]^{-1/2},$$
$$\operatorname{tg}\vartheta_0 = \delta(a_0, \varphi_x)/\Delta(a_0, \varphi_x). \tag{21}$$

The effective damping δ and mismatch Δ are given by Eqs. (15). We can apply the Routh-Hurwitz criterion to the linearized equations (6) to analyze the stability of the steady-state values (a_0, ϑ_0). The necessary and sufficient condition for stability is that

$$\delta_1 + \delta_0 \geqslant 0, \quad \delta_1\delta_0 + \Delta_0\Delta_1 \geqslant 0. \tag{22}$$

We can formally find the zones of instability (i.e., the admissible values of the coupling k and mismatch ξ) by calculating the parameters appearing in (22); however, in order to facilitate the interpretation of the processes involved it is helpful to analyze the evolution of the radio-frequency *V-I* characteristic $a_0 \equiv f(\varepsilon_0)$ in more detail.

In general, numerical methods are needed to calculate the functions in (21). However, the curve $a_0 = f(\varepsilon_0)$ can be analyzed qualitatively under some simplifying assumptions. We can do this by approximating the Kurkijarvi-Webb function by a Z-characteristic (no fluctuations, $\Delta a = 0$), i.e.,

$$P_{KW}(a - b^+) = U(a - b^+), \qquad U(x) = \begin{cases} 0, & x < 0, \\ 1/2, & x = 0, \\ 1, & x > 0. \end{cases}$$

It is also helpful to choose constant biases $\varphi_x = \pi$, so that $b^{\pm} = \pm\varphi_h$ and Eqs. (15) become

$$\delta = (2Q)^{-1}\left[1 + \frac{4k^2Q\varphi_h}{a^2}U(a - \varphi_h)\right],$$
$$\Delta = (2Q)^{-1}\left[\xi + \frac{4k^2Q}{a}(a^2 - \varphi_h^2)^{1/2}U(a - \varphi_h)\right]. \tag{23}$$

Equation (21) for the steady-state amplitude splits into two equations:

$$\varepsilon_0 Q = \begin{cases} a_0(1+\xi^2)^{1/2}, & a_0<\varphi_h=(l^2-1)^{1/2} \\ \{a_0^2(1+\xi^2)+8k^2Q[\varphi_h+2(k^2Q)^2+\xi(a^2-\varphi_h^2)^{1/2}]\}^{1/2}, & a_0\geqslant\varphi_h. \end{cases} \quad (24)$$

This function is shown in Fig. 2; its behavior between the first and second plateaus is fundamentally different for $\xi>0$ and for $\xi<0$. For $\xi>0$ ($\Delta_0>k^2/2$), a_0 depends monotonically on ε_0, which corresponds to the completely stable regime $\partial a/\partial\varepsilon>0$. For negative mismatch $\xi<0$, the dependence is nonmonotonic and the rf V-I characteristic contains a region of decreasing slope with $\partial a/\partial\varepsilon<0$; in this case the steady-state amplitude becomes unstable and a jump will occur to the upper part of the curve. The extremal point (the boundary value for unstable amplitudes) is given by

$$a_m=[\varphi_h^2-4k^2Q\xi/(1+\xi^2)]^{1/2}.$$

The singular points disappear and the curve becomes smooth when fluctuations are allowed for (cf. the dashed curves in Fig. 2). This type of instability is attributable to a violation of the second Routh-Hurwitz condition in (22) (the first condition $\delta_1+\delta_0\geqslant0$ is always satisfied). A direct calculation leads from inequality (22) to an equation for determining the extremal point x_m and the zone of instability, $a_m\geqslant\varphi_h$. In general if the bias is not specially chosen, so that $\varphi_x\neq\pi$ and $b^+\neq|b^-|$, we can find the unstable zone by formally introducing a regeneration coefficient $G\leqslant1$, so that

$$\delta_0\delta_1+\Delta_0\Delta_1=(2Q)^{-2}(1-G)^2. \quad (25)$$

If the interferometer is strongly coupled to the circuit: $4k^2Q/l=\beta\gg1$ and $G\approx1$ then the bound

$$\xi_\beta\leqslant-\{{}^1/_4 Z_0^{-1}(b^+/a)\pm[1+{}^1/_{16}Z_0^{-2}(b^+/a)]^{1/2}\}\beta \quad (26)$$

on the mismatches corresponding to instability is easily found from (25), where

$$Z_0^{-1}=[1-(b^+/a)^2]_0^{-1/2}\approx(l/2\Delta a)^{1/2}.$$

For typical experimental values $l\approx2\pi$ and $\Delta a\approx1/2$, we have $Z_0^{-1}\approx2.5$ and $|\xi_\beta|\lesssim\beta$.

Returning to the physical interpretation of the instability, we should probably point out that the effects of the superconducting interferometer are equivalent to adding a negative resistance to the circuit. According to (25), the nonlinear damping $\delta(a,\varphi_x)$ decreases as the amplitude grows. For constant hysteresis losses $\sim I_0\Phi_0$ beyond the first plateau, an increase in the amplitude is equivalent to a decrease in the dissipative forces. A similar situation occurs for oscillating systems excited by instantaneous forces (such systems were studied in detail in Ref. 15).

4. INFLUENCE OF OSCILLATIONS OF THE SENSITIVITY OF A HYSTERESIS SQUID

In principle, the parametric instability of the steady-state oscillations outside the plateau described above can be used in practice to improve the sensitivity of hysteresis Squids to magnetic fields so that the sensitivity approaches the maximum possible (i.e., is limited only by fluctuations in the Josephson contact itself). This assertion is in fact suggested by the general theory of fluctuations in arbitrary linear dynamic systems.[16] If we consider the combination of the rf Squid and measuring instrument (including the preamplifier stage) as an rf circuit consisting of two noisy four-ports, we have the following expression for the equivalent noise temperature of the entire circuit:

$$T_{\text{eff}}=T_1+T_2/K_{p1}.$$

Here T_1 and T_2 are the equivalent noise temperatures of the Squid and measuring instrument, respectively, and K_{p1} is the transfer coefficient of the Squid (the output signal divided by the input signal at the rated power). For conventional quantum interferometers operating on the plateau, the feedback reaching the oscillating circuit is negative because K_{p1} is always <0, and the noise in the measuring device therefore plays the key role in determining the Squid sensitivity. The dynamic instability associated with off-plateau operation tends to increase the transfer coefficient K_{p1} abruptly; for a highly regenerative Squid with $G\to1$ and $K_{p1}\approx(1-G)^{-2}$, the Squid sensitivity should be independent of the instrument noise and should be limited only by the fluctuations in the circuit and contact. The contact noise will in turn become more important compared to the circuit noise as the factor k^2Q increases (under the usual operating conditions, $k^2Q\approx1$ is optimal). The maximum theoretical Squid sensitivity can thus be approached in principle.

We use Eqs. (8) to calculate the sensitivity quantitatively. It is necessary to calculate the spectral dependences $\overline{|\vartheta_s(\nu)|^2}$, $\overline{|\tilde\vartheta_N(\nu)|^2}$ for the case of phase modulation ($|\tilde a_s(\nu)|^2$, $\overline{|\tilde a_N(\nu)|^2}$ for amplitude modulation), and then take their ratio and integrate over the signal frequency spectrum (this corresponds to optimum selection of the signal from the noise). The smallest recordable signal $\tilde\varphi_s$ can then be estimated by dividing the result of the integration by 2π and equating it to unity.

It is helpful to write out the formulas thus obtained for the following three extreme cases (cf. also Eq. (25) for phase modulation in the regenerative regime outside the plateau, $\beta=4k^2Q/l\gg1$).

I. The noise in the measuring instrument dominates, $T_2>T_1$; in dimensional form, we have the expression

$$(\delta\Phi)^{\mathrm{I}}_{out\,pl}\approx\frac{4}{\beta}(1-G)\left[\frac{\varkappa T_2L_s\Delta a}{\omega\hat\tau}\right]^{1/2} \quad (27a)$$

for the duration $\hat\tau$ of a detectable external signal.

II. The thermal noise of the circuit dominates: $T_1\approx T_c>T_2$. Then

$$(\delta\Phi)^{\mathrm{II}}_{out\,pl}\approx4\left[\frac{\varkappa T_cL_s\Delta a}{\beta\omega\hat\tau}\right]^{1/2}. \quad (27b)$$

III. Most of the noise is from thermal fluctuations in the Josephson contact:

$$\delta\Phi^{\mathrm{III}}_{out\,pl}\approx(0.25-0.5)\Delta a(\omega\hat\tau)^{-1/2}\Phi_0/2\pi. \quad (27c)$$

We have used the fact that

$$\overline{[(\Delta_n^+)^2]}^{1/2}\approx(0.25-0.5)\Delta a.$$

in deriving the last formula.

For comparison, we also note the following formulas[4,11] for the maximum sensitivity for conventional amplitude modulation on the plateau of the V-I Squid characteristic

$(W_0 \approx 1, P_0 \approx 1/2)$:

$$\delta\Phi_{pl}{}^{I} = [2\varkappa T_2 L_s \Delta a/\omega\hat{\tau}]^{1/2}, \quad (28a)$$

$$\delta\Phi_{pl}{}^{II} = [\varkappa T_c L_s (\Delta a)^2/2\omega\hat{\tau}k^2Q]^{1/2}, \quad (28b)$$

$$\delta\Phi_{pl}^{III} = 0{,}5\Delta a(\omega\hat{\tau})^{-1/2}\,\Phi_0/2\pi. \quad (28c)$$

Equations (28a), (28b) imply that the noise in the measuring device dominates on the plateau if $T^2 > T_c(\Delta a/4k^2Q)$. This condition is almost always satisfied, even for maser amplifiers with $T_2 \approx 1-3$ K, because $T_c \approx 4.2$ K, $\Delta a \lesssim 0.5$, $k^2Q \gtrsim 1$, while T_2 is ≈ 100–300 K in most applications.

The instrument/ circuit noise ratio is different for a regenerative Squid operating outside the plateau. Equations (27a, b) show that the noise in the measuring instrument can be neglected unless $T_2 \gg [\beta/(1-G)^2]T_c$, i.e., under these conditions there is an equivalent cooling of the instrument noise by a factor of $\beta(1-G)^{-2}$, and this noise is suppressed to the level of the thermodynamic fluctuations in the circuit for $\beta \gg 1$, $G \to 1$. Since these fluctuations are amplified along with the signal during the recording process, G does not appear in Eq. (27b). Equation (27b) also implies that the only way of effectively suppressing the thermal noise in the circuit is to increase the factor β; for $\beta > 16\kappa TL_s/(\Phi_0/2\pi)^2$ the circuit noise is decreased to the noise level in the Josephson contact, and the Squid sensitivity approaches the limiting value (27c).

5. CONCLUSIONS

Quantum radio-frequency interferometers (Squids) can be regarded as circuits with internal feedback. For conventional Squids operating on the plateau of the V-I characteristic, the feedback is negative and stabilizes the circuit. In the new "off-plateau" regime, the operating point lies between adjacent plateaus and the feedback is positive; a negative conductivity is introduced into the circuit, and regeneration can occur in which the noise temperature of the negative resistance is low and depends only on the physical temperature of the contact. The specific time-dependent behavior of an off-plateau interferometer has much in common with the dynamic properties of classical nonlinear systems excited by instantaneous forces (e.g., self-excited oscillators with a Z-characteristic, the internal mechanisms of clocks, etc.). In discussing the limitations of the results derived above, we note that the above linearized theory rests on the assumption that the variations in the amplitude and phase of the output signal are small compared to the steady-state values: $[\overline{\tilde{a}_N^2}]^{1/2} \ll a^0 \approx l$, $[\overline{\tilde{\vartheta}_N^2}]^{1/2}$. Using the Wiener-Khinchin theorem, we find readily from (8) and (9) that

$$\beta^3 N_1\rho/(1-G)^2 \ll I_0\Phi_0. \quad (29)$$

For the thermal fluctuations in the circuit $N_1 = 2\kappa T/R$ we

$$\frac{1-G}{\beta} \gg \left(\frac{k^2}{l}\frac{\varkappa T}{I_0\Phi_0}\right)^{1/2}. \quad (30)$$

If the noise sources in the system are matched (cf. above), condition (29) leads to

$$\beta \ll [\Phi_0 I_0 Q/\varkappa T_2]^{1/2}, \quad (31)$$

for noise in the measuring device. If the noise temperature T_2 of the measuring device is specified, we can thus find an upper bound for the coupling $\beta = 4k^2Q/l$ from (31) and then use (30) to get a rough upper bound for the regeneration factor G. For the typical values $Q \approx 10^2$, $T \approx 4.2$ K, $T_2 \approx 100$ K, $l \approx 2\pi$, and $I_0 \approx 10^{-4}$ A, conditions (30), (31) are satisfied if $1 - G \geqslant 0.86$ and $\beta \lesssim 20$.

In conclusion, we express our thanks to V. B. Braginskiĭ and V. V. Migulin for a helpful discussion.

[1] I. O. Kulik and I. K. Yanson, The Josephson Effect in Superconducting Tunnel Structures [in Russian], Nauka, Moscow (1970).
[2] J. Clark, Science **216**, 1086 (1982).
[3] B. V. Vasil'ev and E. V. Kolycheva, Zh. Eksp. Teor. Fiz. **74**, 466 (1978) [Sov. Phys. JETP **47**, 243 (1978)].
[4] A. V. Gusev and V. N. Rudenko, Zh. Eksp. Teor. Fiz. **74**, 819 (1978) [Sov. Phys. JETP **47**, 428 (1978)]; **72**, 1217 (1977) [Sov. Phys. JETP **45**, 637 (1977)].
[5] H. J. Paik, Nuovo Cimento **55B**, 15 (1980).
[6] B. V. Vasil'ev and E. V. Kolycheva, Zh. Eksp. Teor. Fiz. **75**, 9 (1978) [Sov. Phys. JETP **48**, 4 (1978)].
[7] F. Everitt, in: Proc. Enrico Fermi School of Physics, Course 56 (B. Bertotti, ed.), Academic Press, Italy (1976).
[8] K. K. Likharev and B. T. Ul'rikh, Systems with Josephson Junctions [in Russian], Izd. Mosk. Gos. Univ. (1978).
[9] V. I. Shnyrkov, Zarubezhnaya Elektron. **6**, 16 (1983).
[10] V. A. Krysanov, A. F. Popkov, and V. I. Rudenko, Preprint No. 16/1983, Mosk. Gos. Univ., Moscow (1983).
[11] V. V. Danilov and K. K. Likharev, Radiotekh. Elektron. **25**, 1725 (1980).
[12] S. M. Rytov, Introduction to Statistical Radiophysics [in Russian], Nauka, Moscow (1974).
[13] B. V. Vasil'ev, JINR Preprint No. R-13-80-588 (1980).
[14] S. A. Belonogov *et al.*, Radiotekh. Elektron. **25**, 2639 (1980).
[15] Yu. A. Mitropol'skiĭ, Lectures on Nonlinear Mechanics [in Russian], Nauka, Moscow (1966).
[16] H. A. Haus and R. B. Adler, Circuit Theory of Linear Noisy Networks MIT Press, Cambridge, Mass. (1959).

Translated by A. Mason